Contemporary Engineering Sciences, Vol. 11, 2018, no. 69, 3409 - 3419
HIKARI Ltd, www.m-hikari.com
https://doi.org/10.12988/ces.2018.87345

Effect of Heat Treatment on the Mechanical Properties of AA2014 Alloy

Abass Ali Saleh

Mustansiriyah University, Faculty of Engineering
Department of Materials Engineering, Baghdad -Iraq

Abstract

AA 2014 wrought Al-alloys of 2xxx series were homogenized followed by heat treatment chiefly involving solutionizing heat treatment, cold deformation rolling and age hardening treatments at specific temperatures for 1–16 h. Their effects were examined in terms of microstructure using SEM analysis and mechanical properties by tensile tests and hardness measurements. The solutionizing and aging treatment done at various temperature namely (503◦C,513◦C.523◦C, and 533◦C) for solution heat treatment and (140◦C, 165◦C, and 190◦C).Deformation ratio of about (2.5%,5%,7.5%) was done on the samples before aging .The changes in hardness and microstructure during heat treatments were determined by traditional material characterization methods. The initial characterizations showed that $CuAl_2$ and AlMnCu and AlMgCu were the primary particles observed in the α-Al matrix. Nearly148 HB hardness was obtained with solutionizing at 513 ◦C and aging at 165 ◦C for 12 h, which was the optimum treatment for obtaining peak hardness. When shaping (deformation) was concerned, a little higher strength and hardness achieved as compared to the non-deformed alloy due to lower strains.

Keywords: AA2014 Aluminum alloy, Precipitation hardening, Deformation, Microstructural characterization

Introduction

Aluminum 2014 alloy responds to heat treatment. It contains copper, manganese, magnesium, and silicon as principle alloying elements. This alloy is vital for aerospace and army vehicle applications. The requirement of aluminum

alloy in the form of sheets with high strength has increased. The strength of the alloy is improved by grain refinement and precipitation hardening techniques significantly [1]. Cryorolling, Friction Stir, The Equal Channel Angular Pressing, Accumulating Roll Bonding, High-Pressure Torsion techniques and Processing are applied for a process the aluminum alloys to develop excellent properties [2].
Corrosion resistance, Formability and outstanding strength vs. density ratio, make age –hardenable aluminum especially series 2xxx alloys high –copper (aluminum-copper-magnesium) alloys a possible candidate for a numeral of industrial uses [3].
In several industrial scopes, Aluminum and its alloys are extensively utilized as appropriate materials for constructions required to be lightened. Aluminum, with more than hundred potential alloying elements, even taking out the elements that are extremely rare or actual poisonous, millions of valuable alloy merging would look potential. Alloying elements are typically an appended to aluminum to enhance its strength, though enhancements in other properties are very vital. The two most frequently utilized methods of improving the strength of aluminum alloys are to:
• Disperse elements in solid solution and cold work the alloy; work hardening alloys,
• Precipitate alloying elements which is dissolved into solid solution as coherent submicroscopic particles: precipitation-hardening alloys [4].
Not as much of investigation has been made to examine age-hardenable alloys likened to non-heat treatable aluminum alloys [5]. Some studies have been made on thermal stability of Al-Cu alloys including extremely fine structure [6]. The potential precipitates in 2xxx series alloys mainly 2014 are $CuAl_2$, $Al_5Cu_2Mg_8Si_5$ and Mg_2Si [7]. The kinetics of grain growth of numerous very fine structures has been discussed that got ready by equal channel angular pressing, cryomillig, and accumulative roll bonding [8].

2- Experimental Work

2.1 Material

The materials used in this research work were wrought 2014 (Al–Cu–Si) heat treatable Al-alloys. It was received in the form of plates of cross section 20 mm x 20 mm. The specimen of the dimensions 15 mm x 10 mm x 10 mm were detached perpendicular to the rolling direction from as received sample Spectroscopic analysis of the alloy was achieved using optical arc emission spectrometer and the composition of the elements is given in Table1.

Table (1).Wrought aluminum alloy composition limits (% weight)

Alloy	Si	Fe	Cu	Mn	Mg	Cr	Zn	Ti	Al
2014	0.81	0.7	4.4	0.8	0.50	0.10	0.25	0.15	Remainder

2.2. Thermal Analysis

Differential scanning calorimetric (DSC) thermal analysis is conducted in the laboratory of Education Ibn Al Haitham Faculty. Samples are selected and cleaned with alcohol and acetone, respectively. The heating rate is chosen as 10∘C/min, and the range of temperature is picked out between 300∘C and 550∘C.

2.3 Heat Treatment

The specimen of wrought 2014 homogenized in electric resistance-type heat treatment furnace at a temperature of 495ºC and eight hours and slowly cooled in the oven to get a uniform reference microstructure. Specimens were then solution heat treated (SHT) to different temperature 503ºC, 513 ºC, 523 ºC, and 533 ºC for one and half hours in order to dissolve all precipitates subsequently quenching in water at room temperature to get a supersaturated solid solution. Thereafter the SHT, the samples were artificially aged in a heating oven at 165ºC (conforming to T6 temper) for a various duration ranging from 1–16 h and water quenched to terminate the further aging reaction. The aged samples were reserved at −5°C in a refrigerator to prevent more aging.

2.4 Cold working process

As a latter step, the influence of the cold worked process preceding to heat treatment was examined. Plates were cold worked with 3 different thicknesses such that nearly 2.5%, 5%, and 7.5% deformation ratio could be established. The deformation process was done at room temperature. The detailed processing of these specimens is tabulated in Table 2.

Table 2. Processing schedule

No.	DEFN %	SOLN		AGING	
		Temp (ºC)	Time (min)	Temp (ºC)	Time (h)
1	-	-	-	-	-
2	-	503	90	165	12
3	-	513	90	165	12
4	-	523	90	165	12
5	-	533	90	165	12
6	-	513	90	140	2,4,6,8,10,12,14,16
7	-	513	90	165	2,4,6,8,10,12,14,16
8	-	513	90	190	2,4,6,8,10,12,14,16
9	2.5	-	-	-	-
10	5	-	-	-	-
11	7.5	-	-	-	-

Table 2. (Continue): Processing schedule

12	2.5	513	90	-	-
13	5	513	90	-	-
14	7.5	513	90	-	-
15	2.5	513	90	165	4,8, 12,16
16	5	513	90	165	4,8, 12,16
17	7.5	513	90	165	4,8, 12,16

2.5 Mechanical Properties

Computation of hardness was done on prepared, flat surface. Brinell hardness numbers were gotten with a 2.5 mm ball indenter under 613 N loads. Three measurements were taken at least for each condition and mean value is repeated in this work. For tensile test, specimens were prepared according to standard of Al tensile test ASTM (B557M-02a).

2.6 Microstructural Examination

Intended for microstructural observations, the surfaces of samples in the solution treated and aged states were made carefully ready by polishing. The samples were polished via emery papers of grits 200, 400, 600, 800 and 1000. The satisfactory polishing was achieved thru utilizing a suspension of 1μm alumina powders in distilled water on a cloth fastened securely to a rotative wheel. The specimens were cautiously washed in order to eliminate all abrasive afterward fine polishing. Keller's reagent (2.5ml HNO_3, 1.5 ml HCl, 1.0 ml HF, and 95 ml Distilled water) are used to etch the samples in order to reveal the grain structure. Afterward, etching specimens were washed in running water and dried. Metallurgical optical microscopes are used to analyze the microstructure at various magnifications.

3. Analyses of Results and Discussion

3.1. Computation of Solution Temperature.

Differential scanning calorimetry (DSC) curve is a mechanism of mensuration for the energy variations between the specimen and the reference material with a change of time and temperature. The curve is founded on the exothermic and endothermic phenomena escorted by the chemical and physical changes happening in the heating process. Next, to the program-controlled temperature, the function link of heat flow rate deviation with temperatures was measured, that is normally used to quantitatively ascertain the melting point and hot melt. From Figure 1, we could locate that the solution temperature is 513 °C.

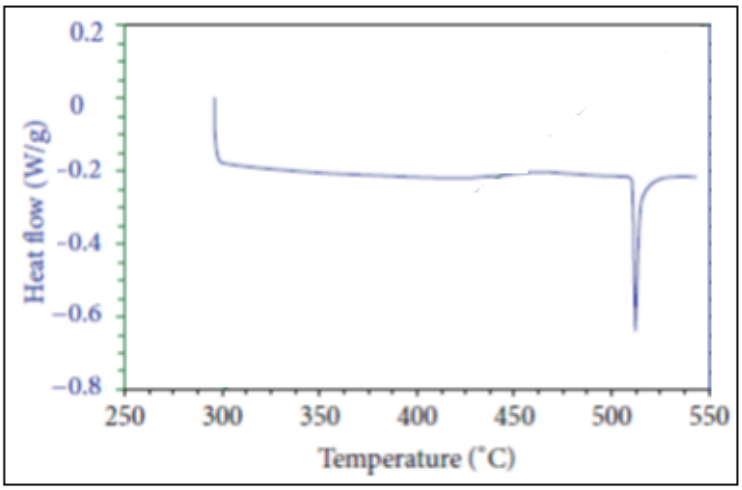

Figure (1) DSC curve for AA2014 alloy

3.2 Ideal heat treatment

The fig.2.represent aging curve shows the response of age hardening treatments on hardness, the difference in hardness with the aging time displayed different peaks conforming to the precipitation of different phases. The presence of distinctive precipitation sequence is evident in an aging curve. A rapid rise in hardness (from solution treated condition, i.e. 105 HV) was realized upon artificial aging up to 4 h which was ascribed to the formation of a coherent zone with the matrix (GP I zone). Additional aging between 4–12 h occasioned in extra hardness raise and peak hardness of about 148 HV loomed in 12 h. Peak hardness in this alloy was a result of precipitation of 2nd phase θ" which is called GP II zone and metastable θ' with the definite crystal structure. Aging for above 12 h have resulted in a progressive reduction in hardness curve owing to over-aging Material becomes soft on account of either coarsening of already precipitated particles or precipitation of equilibrium θ phase which are in-coherent stable precipitates. Thru continued aging at any specified temperature, there is a propensity to dissolve small particles and precipitate larger particles.

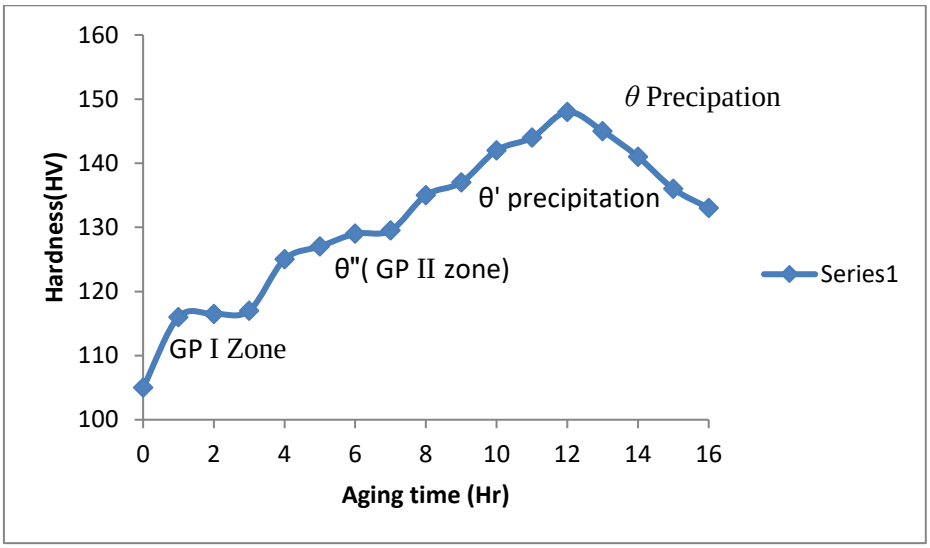

Fig. 2 Hardness Graphs with respect to aging time at 165°C for AA 2014 alloy

The main step for precipitation hardening is Solutionizing heat treatment, and it must be achieved wisely in order to evade grain boundary melting owing to overheating. The influence of solutionizing heat treatment is abridged via a column chart in Figure 3. The as-received AA2014 sample in the annealed temper having a hardness of 105 HB was treated with diverse temperatures and times before artificial aging at 165 ◦C for 12 h. Highest hardness was attained after solutionizing heat treatment at 513 ◦C for 12 h.

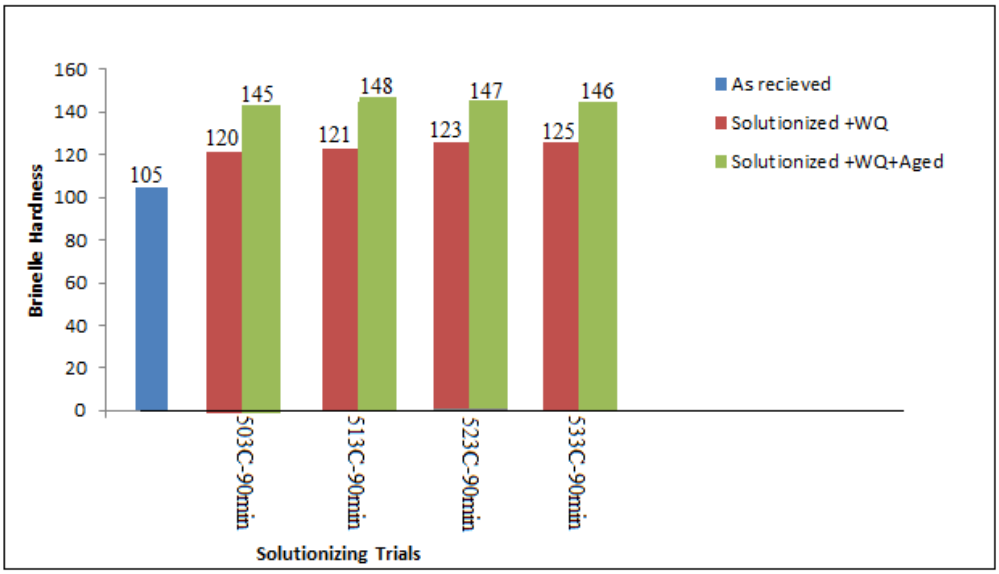

Figure 3. Effect of solutionizing treatment on hardness prior to aging at 165◦C for 12 h.

The aging manner of the AA2014 alloy is potted in Figure 4. It displays distinctive hardness curves of the alloy after solution treating and artificial aging at elevated temperatures. A highest hardness of 148 HB could be achieved after 12 h of aging at 165 ◦C and then the hardness reduced to some extent. The graph for 190 ◦C did not sign peak hardness .The rapid drop in the curve was a sign of the fast overaging owing to extraordinary diffusion rates at high temperatures. Conversely, the influence of slow kinetics could be the deduction of the aging at 140 ◦C. The values of hardness gotten after 16 h could be gained via aging at 165 ◦C for 6 h only. Henceforth it can be settled from Figure 4 that aging at 165 ◦C was the optimum for the alloy, since it yielded the desired hardness values of 135-148HB in 8-12 h.

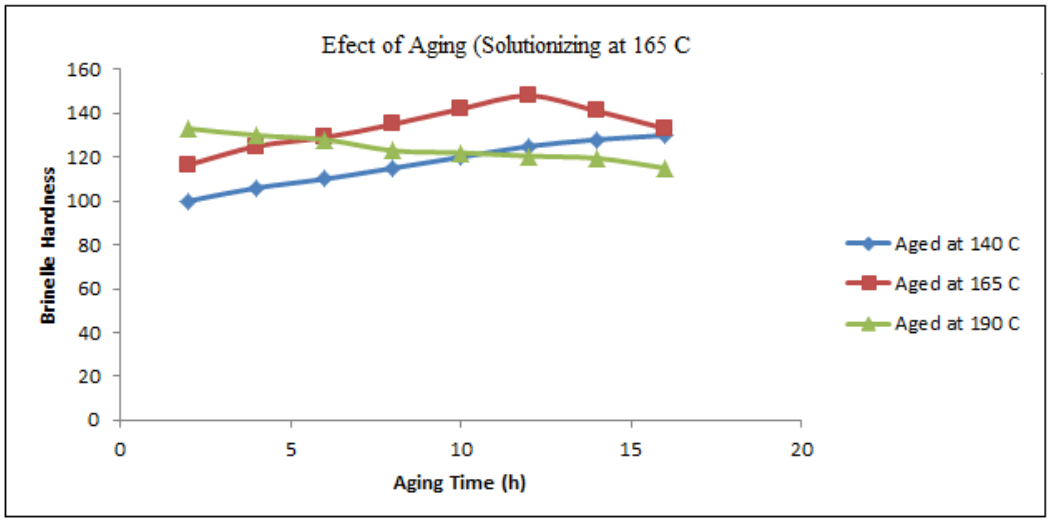

Figure (4).Comparison of aging manner of solutioned alloy aged at temperatures 140,165,190 ^{o} C.

3.3 Microstructural Topographies

The variations in microstructure from solution heat treatment condition to peak hardened condition in reply to aging time can be shown in Fig. 5. Fig. (5a) displays fine re-crystallized grain structure consisting of Aluminum-rich α matrix within which black insoluble coarse particles of AlMnCu and AlMgCu types are existent. These intermetallic particles were not soluble at solution treatment temperature. White, outlined and undissolved $CuAl_2$ precipitates are also observable in the structure. Throughout quenching from solution heat treatment temperature, very fine GP zones and large black particles rosette formed by eutectic melting above the solution annealing temperature. The strain lines are also shown in Fig. 5a. No substantial precipitation was detected in the structure upon artificial aging at 165°C for 5 h. However, less volume of $CuAl_2$ intergranular particles was existing. Precipitates were also found on grain boundaries.

Figure 3b shows the micrograph of sample aged for 8 h containing primarily re-crystallized grains with intragranular precipitation of semi-coherent θ ′ or coherent θ ″ phases. Grain contrast and Strain line were also obvious in the structure. Extraordinary density of fine θ ″ precipitates and θ ′ homogeneously dispersed through the structure was detected in the 12 h aged sample. The fine dispersion (coherent and semi-coherent) of strengthening precipitates is accountable for the greater hardness of the material. In AA 2014, the high copper content (about 4% by wt.) promises the existence of θ precipitation sequence, usually detected for Cu greater than 0.2–0.5 wt.%. Formation of equilibrium θ ($CuAl_2$) phase, which was incoherent with the matrix, occurred after aging above 12 h that is called over-aging. High magnification SEM pictures of the aluminum alloy 2014 samples present in Figure 5. It is clear that the microstructure of 5 h aged sample did not expose any considerable precipitation; Fig. 6a shows only insoluble particles were found at grain boundaries. The virtually clear grains presented that the zones were dissolved and exchanged by coherent fine strengthening precipitates (relatively low amount of θ and mostly θ ″ ′) spread evenly in the matrix. Even though substantial hardness was accomplished after five h aging, nonetheless the precipitates were somewhat so fine that they were not resolved by SEM. Fig. 6b shows fine precipitates with an arrow, both within grains at grain boundaries, found to be consistently distributed through the structure.

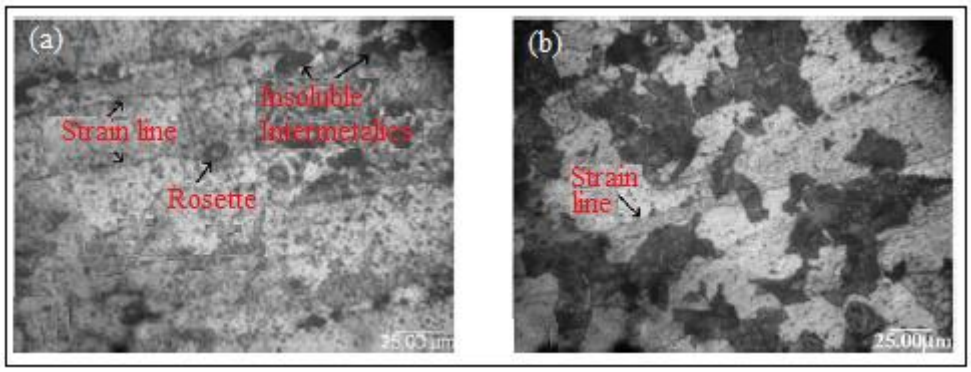

Figure (5) optical micrograph of 2014 aluminum (a) at solution treated (b) after aging for 8 hr

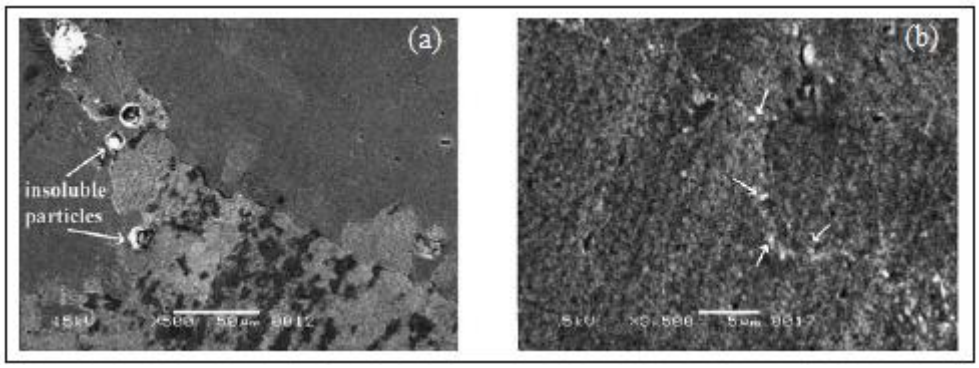

Figure (6) SEM photo for 2014 aluminum alloy selected after (a) aging 5 hr (b) aging 12 hr

3.4 Effect of Deformation

AA 2014 alloy is used in the manufacture of truck frames and aircraft structures. Hence the effect of deformation behavior after solutionizing and prior to aging treatment must be considered. Yield strength ultimate tensile strength (UTS) of deformed and non-deformed specimens after peak aging was achieved from the stress-strain curve and are summarized in Table 3. On the face of it, deformed specimens had a little higher strength as likened to non-deformed ones. The improvement in strength accumulating from the combination of cold working and precipitation heat treating is a consequence of the nucleation of extra precipitate particles via the increased strain. After solution heat treatment and quenching the introduced Strain by cold working also makes nucleation of a finer precipitate dispersion that raises strength. A comparable tendency could be obtained from hardness values. The differences in hardness for non-deformed, 2.5% and 7.5% deformed samples are accessible in Figure 7.

Table 3. Tensile strength of AA2014 alloy solutionized at 513 ◦ C and peak-aged at 165 ◦ C for 12 h after deformation.

Deformation Status	Yield Strength (MPa)	UTS (MPa)
Non-deformed	401	459
2.5% RT	408	466
5 % RT	410	469
7.5 % *RT*	413	473

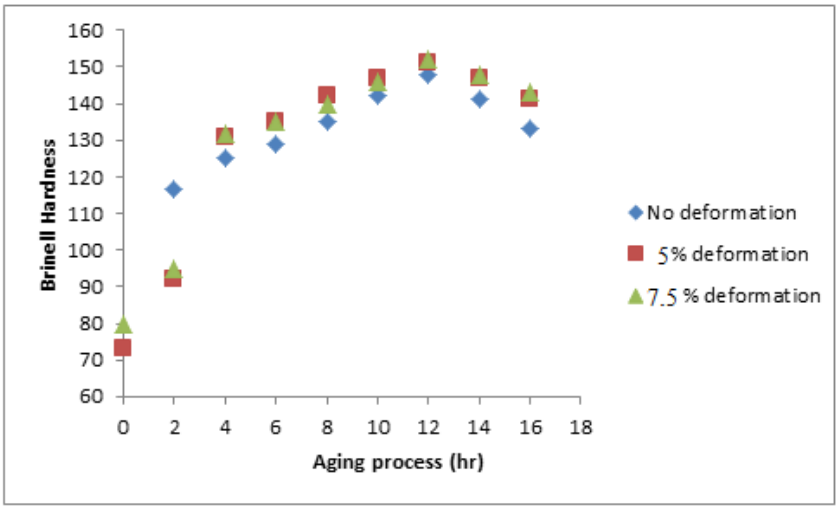

Figure (7) Influence of deformation on the hardness of AA2014 alloy

4. Conclusion

In this paper, the possibility and efficacy of characterizing material properties of aluminum alloy 2014 as a consequence of solutionizing, mechanically deformed by three different deformations ratio (2.5%, 5%, and 7.5%) and then Age hardening treatments for three different temperatures(140°C, 165°C, 190°C) the results, and discussion of this work can be summarized as follows:

1. Samples aluminum alloy 2014 were homogenized, and solution treated followed by artificial aging at various temperatures for variable time durations (1–16 h) to reveal dissimilar steps of precipitation. The best solutionizing temperature was 513 ◦C. Underneath 503 ◦C, there was a trend in the direction of increasing hardness with increasing soaking time.
2. Hardness amounts displayed continuous, non-monotonic increase in hardness in response to aging treatments for aluminum alloy 2014. Upon initial aging, the rapid increase in hardness was observed that was ascribed to the formation of GP zones coherent with the matrix. A small decrease in hardness after a few 2–4 h of aging was owing to the dissolution of GP zones. Hardness reserved increasing till a peak value was reached at the certain aging time. The peak hardness condition is known to be owing to precipitation of semi-coherent and coherent metastable precipitates. Aging for longer times above 12–14 h occasioned in a decrease in hardness owed to dissolution and formation of incoherent precipitates and their coarsening. Aging trials among 140 and 190 ◦C presented that highest hardness values could be gotten after aging at 165 ◦C for 12 h. As linked to the fast overaging at 190 ◦C and slow hardening at 140 ◦C, 165 ◦C was established as the optimal aging temperature for industrial usage.
3. Microstructural variations throughout aging treatments of aluminum alloy 2014 were checked by optical and scanning electron microscopy. The existence of various phases and precipitation sequence lengthways with the over-aging stage was long-established by microscopy, and the consequences were correlated and discussed well with the difference in hardness.
4. It is concluded that as deformation amount ratio increased, the recrystallized grain size got smaller, increasing the strength and hardness.

References

[1] S. Chand, M. D. K. B. Sravani, A. Uma, V. Sindhu, S. P. Devi, G. Padmava, Study OF Microstructure, Hardness and Aging Behaviour of 2014 Aluminum Alloy, *International Journal of Advances in Mechanical and Civil Engineering*, **3** (2016), no. 3, 79-83.

[2] I. Sabirov, M.Y. Murashkin, R.Z. Valiev, Nanostructured aluminium alloys produced by severe plastic deformation: New horizons in development, *Mater. Sci. Eng.: A*, **560** (2013), 1-24. https://doi.org/10.1016/j.msea.2012.09.020

[3] S. Abis, M. Massazza. P. Mengucci and G. Rionio, Early aging mechanisms in a higher-copper AlCuMg Alloys, *Scripta Materialia*, **45** (2001), 685-691. https://doi.org/10.1016/s1359-6462(01)01080-6

[4] E. Atik, C. Meric, B. Karlik, Determination of Yield Strength of 2014 Aluminum Alloy under Aging Conditions by Means of Artificial Neural Networks Method, *Mathematical & Computational Applications*, **2** (1996), 16-20. https://doi.org/10.3390/mca1020016

[5] S.K. Panigrahi, R. Jayaganthan, Effect of Annealing on Thermal Stability, Precipitate Evolution, and Mechanical Properties of Cryorolled Al 7075 Alloy, *Metall. Mater. Trans. A*, **42** (2011), 3208-3217. https://doi.org/10.1007/s11661-011-0723-y

[6] M.A. Nikitina, R.K. Islamgaliev, A.F. Kamalov, Enhanced Thermal Stability and Mechanical Properties of Ultrafine-Grained Aluminum Alloy, *Mater. Sci. Forum*, **667-669** (2011), 331-336. https://doi.org/10.4028/www.scientific.net/msf.667-669.331

[7] P. Bassani, E. Gariboldi, G. Vimercati, Calorimetric analyses on aged Al–4.4Cu–0.5Mg–0.9Si–0.8Mn alloy (AA2014 grade), *J. Therm. Anal. Comp.*, **87** (2007), 247-253. https://doi.org/10.1007/s10973-006-7836-3

[8] K.T. Park, H.J. Kwon, W.J. Kim, Y.S. Kim, Microstructural characteristics and thermal stability of ultrafine grained 6061 Al alloy fabricated by accumulative roll bonding process, *Mater. Sci. Eng. A*, **316** (2001), 145-152. https://doi.org/10.1016/s0921-5093(01)01261-8

Received: August 7, 2018; Published: August 30, 2018